Fault Detection in Continuous Stirred Tank Reactor (CSTR) System Using Extended Luenberger Observer

Dian Mursyitah[1], Putut Son Maria[1], Sovi Pebriani[1], David Delouche[2], Tingting Zhang[3], Frédéric Kratz[4]
[1]Electrical Engineering, UIN Sultan Syarif Kasim, Riau, Indonesia
[2]Automation, JUNIA HEI, Chateauroux, France
[3]Electronic Engineering, Xi'an Shiyou University, Xi'an, China
[4]Automation, INSA Centre Val de Loire, Bourges, France

ARTICLE INFO

Article history:

Received August 14, 2024
Revised November 09, 2024
Published November 30, 2024

Keywords:

Fault diagnosis;
CSTR;
Extended Luenberger Observer;
Robustness;
Sensitivity

ABSTRACT

This research proposes fault detection in a Continuous Stirred Tank Reactor (CSTR) system using an Extended Luenberger Observer (ELO). The ELO is chosen due to the non-linearity of the CSTR system. Accurate state estimation is critical for effective fault diagnosis; therefore, the performance of the ELO is initially tested using two indicators: robustness and sensitivity in estimating the level and concentration within the CSTR system. The sensitivity test yields promising results, with the ELO accurately estimating the actual system despite variations in input and initial conditions, and with a fast convergence time of 1 seconds. The robustness test also demonstrates positive outcomes, as the ELO continues to estimate the system accurately even in the presence of noise with standard deviation 2.5% of measurements. Furthermore, faults that can be related to sensor malfunctions or the disturbances in the CSTR process were successfully detected using the ELO. Performance analysis and fault detection in the CSTR system are presented through simulation. The contributions of this research include development of ELO for non-linear dynamics CSTR system and evidence of its effectiveness in detecting fault within the in CSTR system.

Corresponding Author:

Dian Mursyitah, UIN Sultan Syarif Kasim Riau, HR. Soebrantas, Pekanbaru, Indonesia
Email: dmursyitah@uin-suska.ac.id

1. INTRODUCTION

CSTR are widely employed in various industrial processes due to their efficiency in maintaining a continuous flow and uniform reaction conditions [1]. The CSTR is also plays a pivotal role in wastewater treatment due to its effective mixing, stability, and versatility [2]. However, CSTR system is non-linear and multivariable system, which make them prone to uncertainty. Additionally, like any complex system, CSTRs are susceptible to faults and disturbances that can compromise their performance and safety. To identify faults as they arise and determining the specific type and location of the fault, led us to fault diagnosis. It also includes uncovering one or more root causes of the issues, enabling corrective actions to be implemented [3]. As physical systems become increasingly complex, the need for effective fault diagnosis grows more critical, since it is vital for maintaining system safety and reliability [4]. A key element in fault diagnosis is the residual, defined as the difference between estimated measurements and actual outputs from the system. When the system is fault free, the residual should be zero or close to zero, and otherwise the fault is present [5], [6]. This underscores the importance of accurate state estimation. Fault diagnosis methods are often classified into three big ideas: hardware-based method, model-based method, and historical-based method [7]-[10].

Hardware-based methods rely on additional physical sensors and components to monitor the system's condition, usually is costly. History-based methods, also known as data-driven methods, use historical data and statistical analysis to identify patterns and anomalies indicative of faults, and it depend on the big data. The last term which is model-based methods utilize mathematical models of the system to detect and diagnose faults by comparing the actual system behavior with the expected behavior derived from the model. This method is straightforward, requiring at least a mathematical model of the system, which functions as an observer . Given the non-linearity of many systems, there has been a growing demand for designing non-linear observers that can effectively handle such complexities [5]. In this research, the model-based method is the one we are going to focus on, particularly the non-linear observer method. There are various types of observers which are the Luenberger Observer, High Gain Observer (HGO), Extended Kalman Filter (EKF), Sliding Mode Observer (SMO), and others. As outline in [11] criteria for selecting an observer, focusing on sensitivity to noise and robustness against model errors. The High Gain Observer (HGO) is commonly applied to nonlinear systems, however, selecting the observer gain can amplify disturbances [12], [13] which may obscure information about faults. On the other hand, the Luenberger Observer (LO) is suited for linear systems [14], [15], providing local convergence , while the Extended Kalman Filter (EKF) assumes Gaussian white noise for modeling errors [16]-[18].

Given that the CSTR system's mathematical model is nonlinear, as will be detailed shortly, we opted to utilize Extended Luenberger Observer (ELO). The ELO is a modified or extended versions of LO which is work based on the linear model. Numerous studies have shown the ELO's effectiveness in state estimation and fault diagnosis in the similar systems, such as, three tanks system [19], [20], quadruple-tank [21], heat-exchanger [22], liquid-tanks [23], [24], and other. Its ability to accommodate nonlinearities in system models while maintaining robustness to disturbances makes the ELO particularly suitable for our application in the nonlinear CSTR system. Thus, the ELO stands out as a compelling choice for achieving accurate state estimation and effective fault diagnosis, particularly in CSTR system. Therefore, the main contributions of this research include the development of an ELO specifically designed for the nonlinear CSTR system, offering a novel approach to fault detection. Additionally, this research demonstrates the robustness and sensitivity of the ELO in estimating states accurately under varying conditions, achieving a quick convergence time, and effectively detecting faults even in the presence of noise.

2. METHODS

2.1. CSTR System Mathematical Model

The CSTR system has two inputs: flow rate (F_1) with constant concentration $(C_1)$and flow rate (F_2) with variable concentration (C_2). The output is the flow (F_0) which affects the level in the tank. Assuming that the fluid in the tank is perfectly stirred, the output fluid flow has the same concentration as the concentration in the tank as present in Fig. 1(a). The mathematical representation of the level and concentration in the CSTR are formulated as follows [25]-[27].

$$\frac{dh(t)}{dt} = \frac{1}{A}(F_1 + F_2) - K_c\sqrt{h(t)} \tag{1}$$

$$\frac{dC_0(t)}{dt} = \frac{K_p}{Ah(t)}\Big(\big(C_1(t) - C_0(t)F_1(t)\big) + \big(C_2(t) - C_0(t)F_2(t)\big)\Big) \tag{2}$$

where $h(t)$ is the level of the tank, A is the cross-section area, $F_{in} = F_1 + F_2$ is the input flowrates. K_c and K_p a mixer constant and gap constant, respectively. We can see the parameter of the CSTR system in Table 1.

Table 1. Parameters of CSTR System

Parameters	Value, Symbol, and Unit		
	Value	Symbol	Unit
Flow rate 1	0.6	F_1	(m^3/s)
Flow rate 2	0.15	F_2	(m^3/s)
Volume	1	V	(m^3)
Cross section	1	A	(m^2)
Mixer constant	0.2	K_c	(SI)
Gap constant	0.2	K_p	(SI)
Concentration 1	1	C_1	($Kmol^3$/sec)
Concentration 2	1.2 – 1.4	C_2	($Kmol^3$/sec)

The CSTR system is a coupled system, which refers to a system in which multiple variables or states are interconnected and influence one another [28], [29]. In CSTR, the state that interconnected are the level and concentration. Therefore, if the first input experiences a disturbance, the second output will also be directly affected by this disturbance, and vice versa. To eliminate this coupled influence, a decoupler is designed [30].

The block diagram of the CSTR system with a decoupler is shown in Fig. 1(b). The decoupler designed to ensures that if there is a disturbance in the F_{in} only affects the level output, while a disturbance in the C_{in} only affects the concentration output. This separation simplifies the observer design, as it allows for independent state estimation for each output without interference from the other.

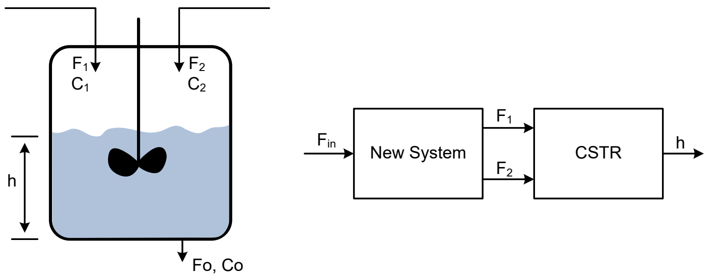

(a) (b)

Fig. 1. (a) CSTR System (b) Diagram block of Decoupler

Fig. 1(a) shows the physical of the CSTR system, while Fig. 1(b) show the block diagram of the decoupler for the CSTR system. The designed decoupler is mathematically represented by rewriting equations (1) and (2). Based on the obtained mathematical model of the system, we can proceed to design of ELO for state estimation.

$$\frac{dh(t)}{dt} = \frac{1}{A}F_{in}(t) - K_c\sqrt{h(t)} \tag{3}$$

$$\frac{dC_0(t)}{dt} = \frac{K_p}{Ah(t)}\left(C_{in}(t)F_{in}(t) - C_0(t)F_{in}(t)\right) \tag{4}$$

where,

$$F_{in}(t) = F_1(t) + F_2(t) \tag{5}$$

$$C_{in}(t) = \frac{C_1(t)F_1(t) + C_2(t)F_2(t)}{F_1(t) + F_2(t)} \tag{6}$$

2.2. The design of Extended Luenberger Observer (ELO)

The ELO is used for non-linear systems [31]-[33]. To better understand the ELO, we begin by modelling the CSTR system using equation (3) and (4). The non-linear CSTR system can be written as the following equation:

$$\begin{aligned} \dot{x}(t) &= f(x,u,t) \\ y(t) &= Cx(t) \end{aligned} \tag{7}$$

where $x \in \mathbb{R}^2$ is the state system, $u \in \mathbb{R}^2$ is the input signal, and $y \in \mathbb{R}^2$ is the output of the system. The non-linear function $f(\cdot)$ related to state x, input signal u, and time t, are described below:

$$f(x,u,t) = \begin{bmatrix} \frac{1}{A}\left(u_1(t) - K_c\sqrt{x_1(t)}\right) \\ \frac{K_p}{Ah}\left(u_2(t)u_1(t) - x_2(t)u_1(t)\right) \end{bmatrix} \tag{8}$$

and the matrix C is presented as follows:

$$C = \begin{bmatrix} 1 & 0 \\ 0 & 1 \end{bmatrix} \tag{9}$$

The ELO algorithm is presented as follows:

$$\dot{\hat{x}}(t) = A(t)\hat{x}(t) + K(t)\big(y(t) - C\hat{x}(t)\big) \tag{10}$$

where $\hat{x} \in \mathbb{R}^2$ is the state estimation, the observer gain $K(t)$ varies with time to ensure precise state estimation and is design based on the linearized system. The choice of observer gain $K(t)$ plays a crucial role in achieving accurate and fast error reduction during the estimation process [34], [35]. The dynamics of the error $e(t) = x(t) - \hat{x}(t)$, can be described as $\dot{e}(t) = \big(A(t) - K(t)\big)e(t)$. The matrix must be chosen such that $(A(t) - K(t)C)$ is stable. This linearized representation allows for the utilization of well-established techniques like pole placement to shape the observer's behavior to guide the selection of $K(t)$. By employing a first-order Taylor expansion and computing the Jacobian matrix [36], the time-varying matrix $A(t)$ is obtained by:

$$A(t) = \left.\frac{\partial f(x,u,t)}{\partial x}\right|_{x=\hat{x}} = \begin{bmatrix} -\dfrac{K_c}{2\sqrt{x_1(t)}} & 0 \\ -\dfrac{K_p}{Ax_1^2(t)}\big(u_2(t)u_1(t) - x_2(t)u_1(t)\big) & \dfrac{K_p}{Ax_1(t)} \end{bmatrix} \tag{11}$$

The design of ELO shown in Fig. 2. In Fig. 2, the gain observer $K(t)$ obtained using pole placement, allowing the determination of a suitable gain to achieve accurate state estimation. In the next section, we present the simulation results along with their analysis. The results illustrate the performance of the ELO in accurately estimating the states of the CSTR system under various operating conditions. Additionally, we discuss the impact measurements noise for estimation.

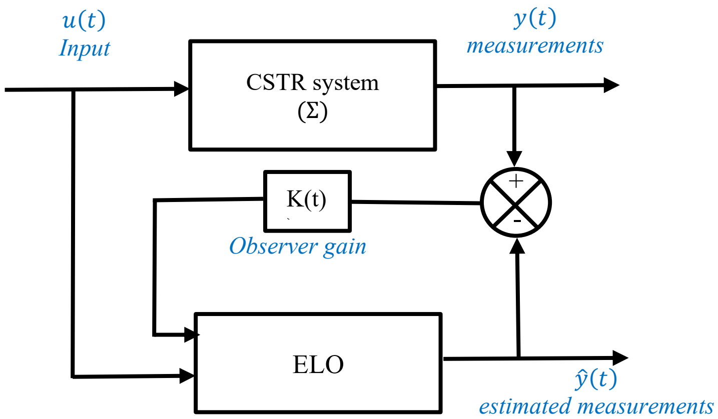

Fig. 2. The block diagram of ELO [37]

3. RESULTS AND DISCUSSION

3.1. State estimation performance

The simulation was conducted using a sampling time $T_s = 0.1$ s and a simulation duration of *50 s*. The input signal was set to a constant value $F_{in} = 0.75m^3/s$ and $C_{in} = 1.27kmol^3/s$. The simulation is shown in Fig. 3(a).

Fig. 3(a) depicts the behavior of the CSTR system. The input signal, referred as F_{in}, is determined by adding F_1 and F_2 as described in equation (5), while C_{in} is defined in equation (6). It is evident that upon applying the input ($F_{in} = 0.75m^3/s$), the system output i.e., level stabilizes at $h = 0.39m$ within 5s. The concentration behaviour is different from level, while the input ($C_{in} = 1.27kmol^3/s$), the output stabilizes within 50 seconds of simulation. Based on the design in (10), the state estimation with ELO is conducted using same sampling and simulation time. The observer gain chosen for this scenario is:

$$K_\infty = \begin{bmatrix} 1.99 \times 10^3 & 0.0281 \\ 0 & 3 \times 10^3 \end{bmatrix} \tag{12}$$

The simulation is shown in Fig. 3(b). It seen that the estimation of level and concentration given by ELO accurately reflects the real state. This alignment between the estimated and actual level and concentration signifies the accuracy of the estimation process with error of estimation consistently at zero. This further validates the precision of the ELO in accurately estimating the system's state

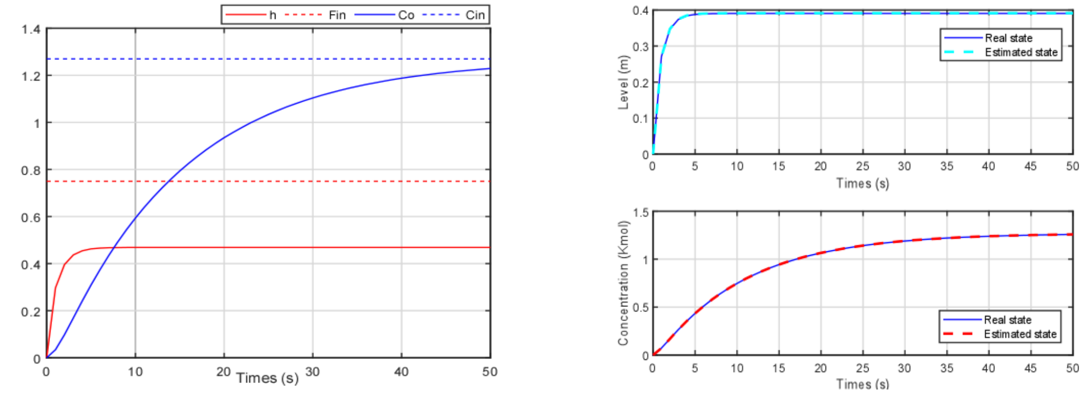

(a) (b)

Fig. 3. (a) Input signal (b) Output level and concentration of CSTR system

3.2. Sensitivity analysis

To conduct sensitivity analysis for the ELO, our next step involves modifying both the input signal to different operating points and adjusting the initial conditions for the ELO. This approach aims to evaluate the observer's sensitivity under varying operating conditions. By systematically testing the observer's performance against different operating points, we aim to further validate its effectiveness in maintaining accurate estimations. This analysis will help demonstrate the ELO's potential for real-time applications.

3.2.1. State estimation performance with different input signal

We initiate the validation process by modifying the input signal, as illustrated in. The input signal undergoes an alteration, transitioning from zero to $F_{in} = 0.75m^3/s$ at 10 second with the step shape. While the concentration input signal is change at 20 second from zero to $C_{in} = 1.27kmol^3/s$. The inputs signals are shown in Fig. 4(a). The operating point is change two times at $t = 0$ and $t = 10s$.

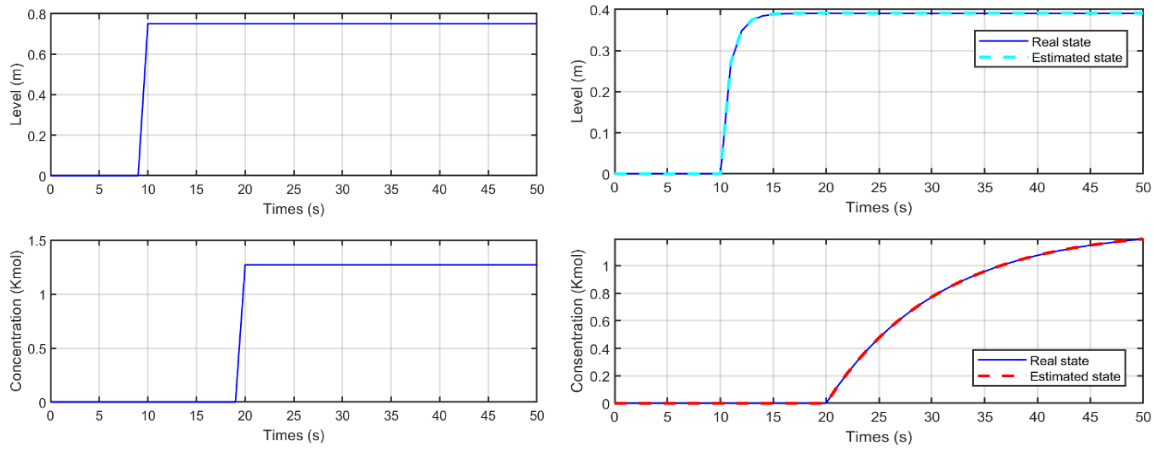

(a) (b)

Fig. 4. (a). Inputs signal in CSTR system with different operating point (b) ELO state estimation system with different operating point in input signal

This deliberate adjustment aims to assess the observer's response and adaptability to different operation point in the CSTR system. In Fig. 4(b) it is evident that the ELO maintains its ability to accurately estimate the true state and track changes in the input. In Fig. 4(a), the input is altered at 10 seconds in accordance with the input signal level, and 20 seconds in the input signal concentration. The convergence time is rapid, as the estimation quickly converges to the actual state from the initial conditions. Remarkably, these consistent results are achieved while maintaining the same initial conditions for both the system and the ELO. This simulation reflects real implementation scenarios where the input signal may not always be constant due to variability.

The subsequent analysis will offer valuable insights into the ELO's capability to accurately estimate system dynamics when the initial conditions are changed. Understanding the impact of initial condition variations on the observer's performance is crucial for assessing its sensitivity [38], [39]. We aim to determine whether the state estimation converges to the actual state even when starting from different initial conditions.

3.2.2. State estimation performance with different initial conditions

To further validate the sensitivity of the ELO, we introduce a change in the initial conditions. In this validation, the initial condition for the system is set to 0, while the ELO's initial condition is set to 1. The results of the state estimation under these adjusted initial conditions are presented in Fig. 5.

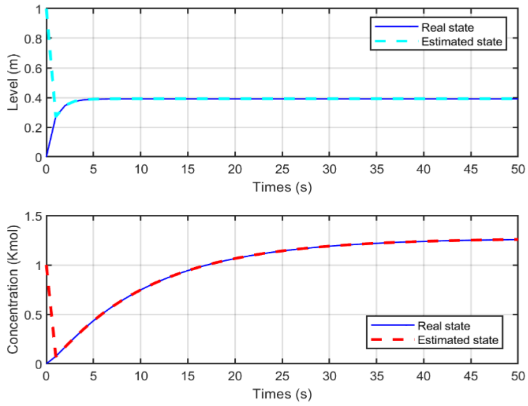

Fig. 5. ELO state estimation of with different initial condition in CSTR system

According to Fig. 5, ELO exhibits no issues related to initial conditions when estimating the level and concentration in the CSTR system. Despite the introduction of different initial conditions, the estimation consistently yields favorable results. It seen in Fig. 5, both the level and concentration estimates converge to the actual state within *1s*, with a total simulation time of *50 s*, indicating fast convergence. To further assess the robustness of our proposed ELO, the next phase of simulation focuses on evaluating its performance with respect to measurement noise.

3.3. Robustness analysis with respect to measurement noise

In this subsection, the validation of robustness is realized by introducing noise into the measurements. We describe the noise as $v \sim \mathcal{N}(0, R)$, where R is presented as follows:

$$R = \begin{bmatrix} 9.4 \times 10^{-4} & 0 \\ 0 & 9.4 \times 10^{-4} \end{bmatrix} \tag{13}$$

The choice of noise is set at a standard deviation of 2.5% of the measurement to ensure that the noise is small enough to avoid overwhelming the system while still being realistic for practical scenarios. Fig. 6 displays the simulation result of state estimation with noisy measurements.

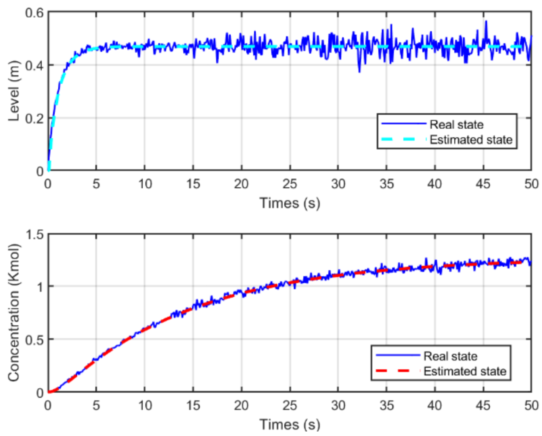

Fig. 6. The ELO estimation with noisy measurements

Fig. 6 present how resistant ELO is against noisy measurement. The estimation of the state continues to follow the trajectories of the true state even in the presence of noise. These results indicate that the estimation performs well under these conditions. While noisy measurements introduce challenges, ELO does not encounter difficulties in estimation on both level and concentration in CSTR system.

3.4. Fault Detection with ELO in CSTR System

The main objective of this research is to detect fault in CSTR. The signal fault is added to flow input F_{in}. Therefore, the fault is set as $f(t) = 5m^3/s$ starting at 10 s to 20 s with ramp shape as shown in Fig. 7(a).

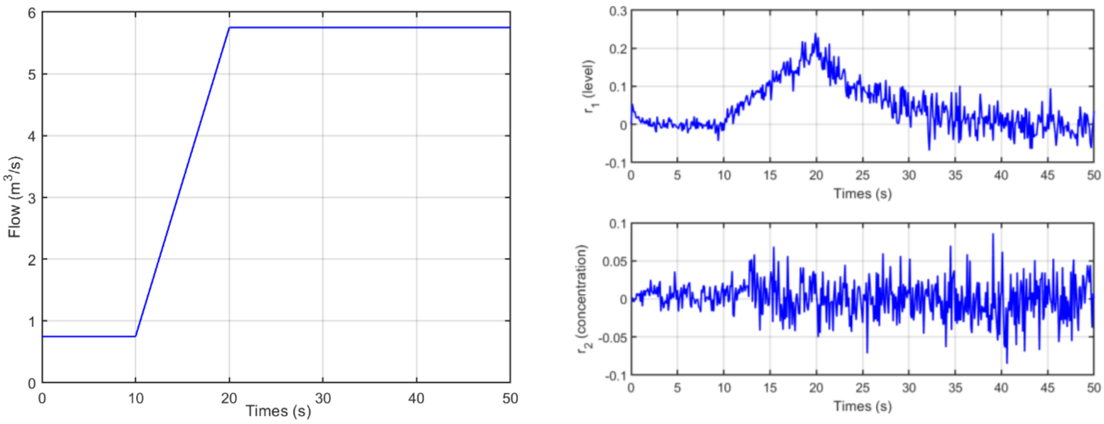

(a) (b)

Fig. 7. (a) Fault signal (b) Residuals

The detect fault, the residual $r(t) = y(t) - C\hat{x}(t)$ is used as fault indicator [40]. The robustness to noise is a critical aspect of this analysis. It is important to consider the noise levels tested in relation to real-world scenarios. The chosen noise levels, with a standard deviation of 2.5% of the measurement, are intended to mimic realistic conditions. In many CSTR systems, typical measurement noise can vary, but levels around 1% to 5% are common due to factors like sensor accuracy and environmental conditions. Therefore, the selected noise levels in this study are representative of typical measurement noise, striking a balance between being realistic and challenging enough to assess the performance of the ELO.The result is shown in Fig. 7(b), where it can be seen that the fault was successfully detected in the first residual, corresponding to the level, as expected since the fault was introduced only in the inlet flow rate (F_{in}). The fault signal in the first residual is visualized as a ramp shape, consistent with the scenario. Based on these results, we can conclude that the ELO is effective for both state estimation and fault diagnosis in the CSTR system. Although the ELO shows robustness at the tested noise level (2.5% of the measurement), higher noise levels may significantly impact its performance, indicating a need for further research.

The results of this study can have significant implications for real-world CSTR systems and similar processes. Implementing the ELO in industrial settings could provide several benefits, including the ELO can enhance the accuracy of state estimations (e.g., level and concentration) in real time, enabling better process control and optimization. The observer's ability to estimate system states can also aid in early fault detection, allowing for maintenance and reducing downtime. The robustness demonstrated against measurement noise ensures that the observer can function effectively in the often-noisy environments of industrial processes.

4. CONCLUSION

In this study, ELO has been designed for state estimation and fault detection in CSTR systems. This research represents the first application of the ELO specifically for state estimation and fault detection in CSTR systems. Fault detection relies on accurate and robust system estimation against disturbances. Therefore, an evaluation of ELO's performance in level and concentration estimation is conducted first. Simulation and analysis results demonstrate ELO's strong performance in estimation, as indicated by sensitivity and robustness to measurements noise. ELO exhibits high sensitivity, providing accurate estimation even with varying inputs and converging to the real system despite differences in initial conditions. Moreover, ELO shows robustness to measurement noise. Finally, fault detection using ELO is successful, accurately identifying simulated fault in the CSTR system. This success underscores ELO's potential as an effective tool for fault detection and anticipation in multivariable non-linear systems CSTR, particularly in industrial applications requiring precise monitoring.

Acknowledgments

The authors would like to thank FITO ALFARIDO and YUDI FARIZTIAWAN for their assistance in completing this research. We would also like to acknowledge the State Islamic University of Sultan Syarif Kasim Riau for their financial support (Grant No: 158/Un.04/L.I/TL.01/03/2024) as of March 1, 2024.

REFERENCES

[1] A. Simorgh, A. Razminia, and V. I. Shiryaev, "System identification and control design of a nonlinear continuously stirred tank reactor," *Mathematics and Computers in Simulation,* vol. 173, pp. 16-31, 2020. https://doi.org/10.1016/j.matcom.2020.01.010.

[2] P. T R *et al.*, "Impact of sludge density and viscosity on continuous stirred tank reactor performance in wastewater treatment by numerical modelling," *Journal of the Taiwan Institute of Chemical Engineers,* p. 105368, 2024, https://doi.org/10.1016/j.jtice.2024.105368.

[3] A. Diedrich and O. Niggemann, "On Residual-based Diagnosis of Physical Systems," *Engineering Applications of Artificial Intelligence,* vol. 109, p. 104636, 2022/03/01/ 2022, https://doi.org/10.1016/j.engappai.2021.104636.

[4] H. R. Chavoshi, A. K. Sedgh, M. A. Shoorehdeli, and H. Khaloozadeh, "Practical Implementation of Multiple Faults in a Coupled-Tank System: Verified by Model-Based Fault Detection Methods," in *2023 11th RSI International Conference on Robotics and Mechatronics (ICRoM)*, pp. 488-493, 2023, https://doi.org/10.1109/ICRoM60803.2023.10412498.

[5] S. Venkateswaran, Q. Liu, B. A. Wilhite, and C. Kravaris, "Design of linear residual generators for fault detection and isolation in nonlinear systems," *International Journal of Control,* vol. 95, no. 3, pp. 804-820, 2022, https://doi.org/10.1080/00207179.2020.1823020.

[6] A. Mouzakitis, *Classification of Fault Diagnosis Methods for Control Systems* (Measurement and Control, no. 10). SAGE Publications Ltd, 2013, pp. 303-308. https://doi.org/10.1177/0020294013510471.

[7] R. Arunthavanathan, F. Khan, S. Ahmed, and S. Imtiaz, "An analysis of process fault diagnosis methods from safety perspectives," *Computers & Chemical Engineering,* vol. 145, p. 107197, 2021, https://doi.org/10.1016/j.compchemeng.2020.107197.

[8] V. Venkatasubramanian, R. Rengaswamy, K. K. Yin, and S. N. Kavuri, "A review of process fault detection and diagnosis: Part I: Quantitative model-based methods," *Comput. Chem. Eng.,* vol. 27, pp. 293-311, 2003, https://doi.org/10.1016/S0098-1354(02)00160-6.

[9] D. Li, Y. Wang, J. Wang, C. Wang, and Y. Duan, "Recent advances in sensor fault diagnosis: A review," *Sensors and Actuators A: Physical,* vol. 309, p. 111990, 2020, https://doi.org/10.1016/j.sna.2020.111990.

[10] M. M. Syed, T. A. Lemma, S. K. Vandrangi, and T. N. Ofei, "Recent developments in model-based fault detection and diagnostics of gas pipelines under transient conditions," *Journal of Natural Gas Science and Engineering,* vol. 83, p. 103550, 2020, https://doi.org/10.1016/j.jngse.2020.103550.

[11] G. Graton, J. Fantini, and F. Kratz, "Finite Memory Observers for linear time-varying systems. Part II: Observer and residual sensitivity," *Journal of the Franklin Institute,* vol. 351, no. 5, pp. 2860-2889, 2014, https://doi.org/10.1016/j.jfranklin.2013.12.022.

[12] X. Meng, H. Yu, J. Zhang, T. Xu, H. Wu, and K. Yan, "Disturbance Observer-Based Feedback Linearization Control for a Quadruple-Tank Liquid Level System," *ISA Transactions,* vol. 122, pp. 146-162, 2022, https://doi.org/10.1016/j.isatra.2021.04.021.

[13] S. M. Mousavi and M. Guay, "A Peaking Free Time-Varying High-Gain Observer With Reduced Sensitivity to Measurement Noise," *IEEE Control Systems Letters,* vol. 7, pp. 2857-2862, 2023, https://doi.org/10.1109/LCSYS.2023.3290045.

[14] R. Mahony, P. Van Goor, and T. Hamel, "Observer design for nonlinear systems with equivariance," *Annual Review of Control, Robotics, and Autonomous Systems,* vol. 5, no. 1, pp. 221-252, 2022, https://doi.org/10.1146/annurev-control-061520-010324.

[15] S. Liu, S. Chen, T. Chen, and Z. Ren, "Residual neural network-based observer design for continuous stirred tank reactor systems," *Communications in Nonlinear Science and Numerical Simulation,* vol. 128, p. 107592, 2024, https://doi.org/10.1016/j.cnsns.2023.107592.

[16] P. S. Madhukar and L. Prasad, "State estimation using extended kalman filter and unscented kalman filter," in *2020 International Conference on Emerging Trends in Communication, Control and Computing (ICONC3)*, pp. 1-4, 2020, https://doi.org/10.1109/ICONC345789.2020.9117536.

[17] M. Khodarahmi and V. Maihami, "A review on Kalman filter models," *Archives of Computational Methods in Engineering,* vol. 30, no. 1, pp. 727-747, 2023, https://link.springer.com/article/10.1007/s11831-022-09815-7.

[18] L. Torres, J. Jiménez-Cabas, O. González, L. Molina, and F.-R. López-Estrada, "Kalman Filters for Leak Diagnosis in Pipelines: Brief History and Future Research," *Journal of Marine Science and Engineering,* vol. 8, no. 3, p. 173, 2020, https://doi.org/10.3390/jmse8030173.

[19] S. Rúa, R. E. Vásquez, N. Crasta, and C. A. Zuluaga, "Observability analysis and observer design for a nonlinear three-tank system: Theory and experiments," *Sensors,* vol. 20, no. 23, p. 6738, 2020, https://doi.org/10.1146/annurev-control-061520-010324.
[20] A. Nasr, I. Khoja, T. Ladhari, and S. H. Said, "Synthesis of Observers for the Three Tank System," in *2023 IEEE International Conference on Artificial Intelligence & Green Energy (ICAIGE)*, pp. 1-6, 2023, https://doi.org/10.1109/ICAIGE58321.2023.10346279.
[21] M. K. Wafi and B. L. Widjiantoro, "Distributed estimation with decentralized control for quadruple-tank process," *International Journal of Scientific Research in Science and Technology* vol. 9, no. 1, pp. 301-307, 2023, https://doi.org/10.3329/bjsir.v57i3.62017.
[22] X. Han, Z. Li, M. Cabassud, and B. Dahhou, "A comparison study of nonlinear state observer design: Application to an intensified heat-exchanger/reactor," in *2020 28th Mediterranean Conference on Control and Automation (MED)*, pp. 162-167, 2020, https://doi.org/10.1109/MED48518.2020.9183148.
[23] V. Shenoy and S. K. Vekata, "Estimation of Liquid Level in a Harsh Environment Using Chaotic Observer," *Journal of Robotics and Control (JRC),* vol. 3, no. 5, pp. 566-582, 2022, http://dx.doi.org/10.18196/jrc.v3i5.16183.
[24] J. D. Avilés, I. Torres-Zúñiga, A. Villa-Leyva, A. Vargas, and G. Buitrón, "Experimental validation of an interval observer-based sensor fault detection strategy applied to a biohydrogen production dark fermenter," *Journal of Process Control,* vol. 114, pp. 131-142, 2022, https://doi.org/10.1016/j.jprocont.2022.04.012.
[25] D. Stavrov, G. Nadzinski, S. Deskovski, and M. Stankovski, "Quadratic model-based dynamically updated pid control of cstr system with varying parameters," *Algorithms,* vol. 14, no. 2, p. 31, 2021, https://doi.org/10.3390/a14020031.
[26] D. Mursyitah, A. Faizal, and E. Ismaredah, "Level Control in Coupled Tank System Using PID- Fuzzy Tuner Controller," *Controls and Informatics Seminar*, pp. 293-298, 2018, https://doi.org/10.1109/EECCIS.2018.8692846.
[27] H. G. Ibrahim, "Mathematical modeling and simulation of control strategies for continuous stirrer tank reactor," *Bangladesh Journal of Scientific and Industrial Research,* vol. 57, no. 3, pp. 149-162, 2022, https://doi.org/10.3329/bjsir.v57i3.62017.
[28] J. K. Pradhan and A. Ghosh, "Design and implementation of decoupled periodic control scheme for a laboratory-based quadruple-tank process," *Proceedings of the Institution of Mechanical Engineers, Part I: Journal of Systems and Control Engineering,* vol. 236, no. 1, pp. 212-224, 2022. https://doi.org/10.1177/09596518211022897.
[29] P. K. Choudhary, D. K. Das, and G. Gurumurthy, "Receding Horizon Controller for Decoupled Two-Input Two-Output Coupled Tank System," in *2022 4th International Conference on Energy, Power and Environment (ICEPE)*, pp. 1-5, 2022, https://doi.org/10.1109/ICEPE55035.2022.9797979.
[30] M. Panneerselvam, S. C. Narayany, M. F. Mariam, K. H. Priya, and K. Narmatha, "Decentralized PID control for nonlinear multivariable systems using decoupler," *International Journal of Nonlinear Analysis and Applications,* vol. 12, no. Special Issue, pp. 1529-1539, 2021, https://doi.org/10.22075/ijnaa.2021.5805.
[31] J. Gauthier, H. Hammouri, and S. Othman, "A simple observer for nonlinear systems applications to bioreactors," *IEEE Transactions on automatic control,* vol. 37, no. 6, pp. 875-880, 1992, https://doi.org/10.1109/9.256352.
[32] G. Besançon, D. Georges, O. Begovich, C. Verde, and C. Aldana, "Direct observer design for leak detection and estimation in pipelines," in *2007 European Control Conference (ECC)*, pp. 5666-5670, 2007, https://doi.org/10.23919/ECC.2007.7068535.
[33] S. Marzougui, S. Bedoui, A. Atitallah, and K. Abderrahim, "Parameter and state estimation of nonlinear fractional-order model using Luenberger observer," *Circuits, Systems, and Signal Processing,* vol. 41, no. 10, pp. 5366-5391, 2022. http://dx.doi.org/10.1007/s00034-022-02031-5.
[34] A. Adil, A. Hamaz, I. N'Doye, A. Zemouche, T.-M. Laleg-Kirati, and F. Bedouhene, "On high-gain observer design for nonlinear systems with delayed output measurements," *Automatica,* vol. 141, p. 110281, 2022, https://doi.org/10.1016/j.automatica.2022.110281.
[35] X. Jia, S. Xu, and S. Zhou, "Adaptive Output Feedback Control of Nonlinear Systems: A Dynamic-Gain Scaling Approach," *IEEE Transactions on Automatic Control,* vol. 68, no. 8, pp. 5150-5157, 2023, https://doi.org/10.1109/TAC.2022.3221905.
[36] M. Asghari, A. M. Fathollahi-Fard, S. M. J. Mirzapour Al-e-hashem, and M. A. Dulebenets, "Transformation and Linearization Techniques in Optimization: A State-of-the-Art Survey," *Mathematics,* vol. 10, no. 2, p. 283, 2022, https://doi.org/10.3390/math10020283.
[37] L. Yousfi, S. Aoun, and M. Sedraoui, "Speed sensorless vector control of doubly fed induction machine using fuzzy logic control equipped with Luenberger observer," *International Journal of Dynamics and Control,* vol. 10, no. 6, pp. 1876-1888, 2022, http://dx.doi.org/10.1007/s40435-022-00946-0.
[38] B. Mu, X. Yang, and J. K. Scott, "Comparison of advanced set-based fault detection methods with classical data-driven and observer-based methods for uncertain nonlinear processes," *Computers & Chemical Engineering,* vol. 166, p. 107975, 2022, https://doi.org/10.1016/j.compchemeng.2022.107975.
[39] T. Zhang, "Finite memory observer design for continuous-time nonlinear systems with discrete-time measurements: application to diagnosis," PhD Thesis, INSA Centre Val de Loire, 2021, https://hal.science/tel-03195258/.
[40] D. C. Montgomery, *Introduction to statistical quality control*. John Wiley & Sons, 2020, https://books.google.co.id/books?hl=id&lr=&id=YWLNEAAAQBAJ.

Vol. 10, No. 4, December 2024, pp. 681-690

BIOGRAPHY OF AUTHORS

Dian Mursyitah, Lecturer at UIN Sultan Syarif Kasim Riau. Email: dmursyitah@uin-suska.ac.id.

Putut Son Maria, Lecturer at UIN Sultan Syarif Kasim Riau. Email: putut.son@uin-suska.ac.id.

Sovi Pebriani, Student in UIN Sultan Syarif Kasim Riau, sovipebriani@uin-suska.ac.id.